Depressed Levels of Prostaglandin $F_{2\alpha}$ in Mice Lacking Akr1b7 Increase Basal Adiposity and Predispose to Diet-Induced Obesity

Fanny E. Volat,[1] Jean-Christophe Pointud,[1] Emilie Pastel,[1] Béatrice Morio,[2] Benoit Sion,[3] Ghislaine Hamard,[4] Michel Guichardant,[5] Romain Colas,[5] Anne-Marie Lefrançois-Martinez,[1] and Antoine Martinez[1]

Negative regulators of white adipose tissue (WAT) expansion are poorly documented in vivo. Prostaglandin $F_{2\alpha}$ ($PGF_{2\alpha}$) is a potent antiadipogenic factor in cultured preadipocytes, but evidence for its involvement in physiological context is lacking. We previously reported that Akr1b7, an aldo-keto reductase enriched in adipose stromal vascular fraction but absent from mature adipocytes, has antiadipogenic properties possibly supported by $PGF_{2\alpha}$ synthase activity. To test whether lack of Akr1b7 could influence WAT homeostasis in vivo, we generated $Akr1b7^{-/-}$ mice in 129/Sv background. $Akr1b7^{-/-}$ mice displayed excessive basal adiposity resulting from adipocyte hyperplasia/hypertrophy and exhibited greater sensitivity to diet-induced obesity. Following adipose enlargement and irrespective of the diet, they developed liver steatosis and progressive insulin resistance. Akr1b7 loss was associated with decreased $PGF_{2\alpha}$ WAT contents. Cloprostenol ($PGF_{2\alpha}$ agonist) administration to $Akr1b7^{-/-}$ mice normalized WAT expansion by affecting both de novo adipocyte differentiation and size. Treatment of 3T3-L1 adipocytes and $Akr1b7^{-/-}$ mice with cloprostenol suggested that decreased adipocyte size resulted from inhibition of lipogenic gene expression. Hence, Akr1b7 is a major regulator of WAT development through at least two $PGF_{2\alpha}$-dependent mechanisms: inhibition of adipogenesis and lipogenesis. These findings provide molecular rationale to explore the status of aldo-keto reductases in dysregulations of adipose tissue homeostasis. *Diabetes* 61:2796–2806, 2012

Obesity is the result of genetic predisposition and environmental factors that confer an imbalance between energy intake and energy expenditure (1). Resulting energy excess is stored as triglycerides in white adipose tissue (WAT). Adult obesity is typically characterized by adipocyte hypertrophy when triglyceride synthesis exceeds breakdown (lipolysis). However, a concomitant adipocyte hyperplasia may also occur as a result of increased recruitment and differentiation of precursor cells (adipogenesis) (2,3).

In addition to its role in energy storage, WAT is also a highly active metabolic and endocrine organ that regulates energy homeostasis by secreting a variety of adipokines (4). These factors may act at local (auto/paracrine) or systemic (endocrine) levels and enable WAT to modulate its own metabolic activities or that of other tissues. So, excess or deficiency of adipose tissue may generate metabolic disorders such as liver steatosis, insulin resistance, type 2 diabetes, and cardiovascular diseases.

The use of well-characterized preadipocyte cell lines, 3T3-L1 or 3T3-F442A, allowed us to draw a network of transcription factors regulating differentiation of fibroblast-like preadipocytes to lipid-loaded adipocytes (5,6). Peroxisome proliferator-activated receptor γ and CCAAT/enhancer-binding proteins emerged as master regulators of the transcriptional cascade that drives adipogenesis (7,8). Expression and activity of these transcriptional factors are controlled by various upstream stimuli (hormonal, paracrine, or nutritional), leading to the regulation of adipocyte-specific genes. Therefore, study of the balance between negative and positive regulators of adipogenesis is essential for understanding the early mechanisms involved in the establishment of obesity.

Prostaglandins (PG) are lipid paracrine mediators that were shown to play opposite and sometimes conflicting actions on cultured adipocytes. Therefore, until the recent development of genetically engineered mice models, their physiological importance in adipose tissue homeostasis remained unclear. PGE_2 and PGD_2/PGJ_2 were shown to promote adiposity in mice through inhibition of lipolysis and induction of adipogenesis, respectively (9–11). By contrast, $PGF_{2\alpha}$ is a potent inhibitor of adipocyte differentiation in vitro (12–14). $PGF_{2\alpha}$, via its PGF (FP) receptor, activates downstream signaling pathways involving mitogen-activated protein kinase and/or calcineurin. This leads to inhibition of expression or activity of the proadipogenic transcription factors peroxisome proliferator-activated receptor γ and CCAAT/enhancer-binding protein α (12,15,16). Although the molecular action of $PGF_{2\alpha}$ has been well-described in cell cultures, its role in adipose tissue homeostasis in vivo has not been elucidated so far as the PGF synthases (PGFS) responsible for its production were only recently identified.

Indeed, we showed that some aldo-keto reductase 1B (AKR1B) members exhibited PGFS activity in vitro. Human AKR1B1 and murine Akr1b3 and Akr1b7 catalyze the synthesis of $PGF_{2\alpha}$ from its precursor PGH_2 through

their 9,11-endoperoxide reductase activity (17). Although a recent study indicated that the PGFS activity of Akr1b3 can influence adipogenesis in 3T3-L1 cells (18), no defect in adipose tissue homeostasis was reported in Akr1b3-deficient mice (19). Contrasting with the ubiquitous Akr1b3 protein, Akr1b7 isoform is expressed in a restricted set of tissues (i.e., adrenal glands, reproductive organs, and intestine) (20–23) and was found more recently in the adipose tissue (24). Interestingly, in fat depots, Akr1b7 expression is limited to the preadipocyte-enriched stromal fraction and downregulated during the differentiation into adipocytes (24). Consistently, over-expression of Akr1b7 in 3T3-L1 preadipocytes inhibits their differentiation, whereas Akr1b7 knockdown accelerates the adipogenic program. All of these data show that Akr1b7 exerts an antiadipogenic action in cell culture, although the mechanisms involved and the potential role of its PGFS activity remain to be established. We recently demonstrated that Akr1b7 is able to regulate the stress-induced response of adrenal gland by generating a $PGF_{2\alpha}$ signal in vivo (25). Hence, we hypothesized that the enrichment of Akr1b7 in the adipose stromal fraction could have a key role in preventing adiposity in vivo by controlling $PGF_{2\alpha}$ content. To firmly demonstrate the antiadipogenic action of Akr1b7 and the possible involvement of $PGF_{2\alpha}$ in this process, we generated $Akr1b7^{-/-}$ mice and characterized their phenotype under standard or obesogenic diet conditions. We report that ablation of Akr1b7 increases adiposity under regular diet and decreases metabolic rate. This predisposes mice to develop severe obesity under a high-fat diet (HFD). These phenotypes result from deregulation of both adipogenesis and lipogenesis through a $PGF_{2\alpha}$-dependent mechanism.

RESEARCH DESIGN AND METHODS

Generation of *Akr1b7*-null mice. *Akr1b7* genomic vector was created using PCR-amplified fragments from a phage λ genomic clone containing the whole *Akr1b7* gene. The targeted construct was generated by inserting hygromycine resistance cassette flanked by two loxP sites and a third loxP to flank exons 4–6 (Fig. 1A). The 11-kb targeting fragment was linearized and electroporated into 129/Sv embryonic stem cells. Hygromycine-resistant clones were screened for homologous recombination by Southern blot of *Hind*III-digested DNA with the 5′ untranslated region probe of the *Akr1b7* gene. Chimeric males, obtained by microinjecting positive clones into C57BL/6J blastocysts, were crossed with 129/Sv wild-type (WT) females to screen for germline transmission. Homozygous animals for *Akr1b7^flox-hygro* allele were crossed with mice of the MeuCre40 transgenic line (26) to obtain recombination between loxP1 and loxP3 sites. Mosaic animals containing the *Akr1b7*-null allele lacking exons 4–6 were detected by Southern blotting. They were crossed with 129/Sv WT animals to generate *Akr1b7^+/−* mice. Details on vector construction or genotyping are available on request. *Akr1b7^−/−* mice were born viable at Mendelian frequency and showed no defects in reproductive functions as reported for a previous model of *Akr1b7* knockout (KO) mice (27).

Mice, diet, and treatments. All animal studies were approved by the Auvergne Ethics committee and conducted in agreement with international standards for animal welfare. WT and mutant littermate (KO) males were fed ad libitum a standard diet (Harlan Diet) or a high-fat diet (HFD) (63% kcal fat, 19% kcal carbohydrate, and 18% protein) (U8954, Safe) for either 12 or 5 weeks, respectively. Food intake was measured daily over a 6-day period. For phenotypic rescue studies, *Akr1b7*-null mice were intraperitoneally injected daily with vehicle PBS or cloprostenol (0.1 µg/g/day; Sigma-Aldrich) throughout the duration of HFD protocols. Mice were killed by decapitation, and truncal blood was collected.

Ambulatory activity. Ambulatory activity of 3-, 9-, and 18-month-old mice was recorded with the Activiwheel software (IntelliBio). Mice were housed individually in cages containing an activity wheel (IntelliBio). The recordings of locomotor activity were performed at least on six mice of each genotype. Two recordings of 24 h were performed per mouse.

Indirect calorimetry. Respiratory gas exchanges were measured continuously using whole-body calorimetric chambers (TSE Systems, Bad Homburg

v.d.h., Germany). Energy expenditure was calculated using Weir's equation (28). Respiratory quotient was calculated from the ratio between CO_2 production and O_2 consumption.

Culture of 3T3-L1 cells. 3T3-L1 preadipocytes were induced to differentiate as previously described (24).

Gene expression. RNAs were isolated from mouse tissues or 3T3-L1 cells using TRIzol reagent (Invitrogen), and cDNAs were synthesized with M-MLV reverse transcriptase (Promega). Gene expression was assessed by real-time quantitative PCR (RTqPCR) using TaqMan probes and PCR Mastermix (Applied Biosystems) or SYBR green and standard primers (Supplementary Table 1). Each reaction was performed in triplicate, quantification was performed by the ΔΔCt method, and relative gene expression was normalized to peptidyl-prolyl isomerase B levels (ppib). The following TaqMan probes were used: *Scd1* Mm01197142_m1; *Fasn* Mm01253292_m1; *Acaca* Mm01304257_m1; *Akr1b3* Mm01135578_g1; and *Ppib* Mm00478295_m1.

Plasma and intratissular metabolites. Blood samples were collected after an overnight fasting. Insulin/leptin and adiponectin/resistin (Thermo Fisher Scientific) levels were measured by ELISA kits (BioVendor, Assaypro; both Thermo Fisher Scientific). Plasma concentration of cholesterol, triglycerides (Thermo Fisher Scientific), glycerol, and free fatty acids (Randox) were determined using commercial kits. For intratissular lipids assays, lipids were extracted from livers as previously described (29).

Histology and in vivo bromodeoxyuridine labeling studies. WAT were fixed in 4% paraformaldehyde and embedded in paraffin. Sections (7 µm) were stained with hematoxylin/eosin and images captured for determination of cell surface with ImageJ software (National Institutes of Health). Livers were fixed in 4% paraformaldehyde and cryoprotected in sucrose overnight before −80°C OCT freezing. The 10-µm cryosections were performed at −16°C before Oil Red O staining.

Bromodeoxyuridine (BrdU) was administered to 16-week-old mice by intraperitoneal injection (50 mg/kg) every second day of the last 3 weeks of the 5-week HFD protocol. BrdU labeling was detected on WAT paraffin sections. Deparaffinized sections were incubated 25 min at 95°C in unmasking solution (sodium citrate buffer 10 mmol/L, pH 6, Tween 0.05%) before incubation with 1:50 dilution of mouse anti-BrdU antibody (Roche) revealed by goat anti-mouse Alexa 555 at 1:1000 (Molecular Probes). Sections were then incubated with Hoechst (Sigma-Aldrich), mounted in PBS-glycerol, and photographed on Zeiss LSM 510 Meta Confocal microscope (Carl Zeiss).

Immunoblotting. Proteins (20–40 µg) were loaded on SDS-PAGE, transferred onto nitrocellulose, and detected with the following antibodies: rabbit anti-Akr1b7 (L4; 1:5,000), rabbit anti-Akr1b3 (L5; 1:2,000), rabbit anti-Akr1b8 (L7; 1:2,000) (25), rabbit anti-Akt (Cell Signaling Technology; 1:1,000), rabbit anti–p-Akt ser473 (Epitomics; 1:3,000), rabbit anti-FP receptor (Cayman Chemical; 1:500), mouse anti–Srebp-1 (Thermo Scientific; 1:200), rabbit anti–β-actin (Sigma-Aldrich; 1:5,000), or mouse anti–β-tubulin (Sigma-Aldrich; 1:1,000).

Glucose and insulin tolerance tests. These tests were performed on 14- and 5-h fasted mice, respectively. Blood glucose concentration was measured from the tail vein at 0, 15, 30, 60, 90, and 120 min after intraperitoneal injection of glucose (2 g/kg body weight) or insulin (0.75 units/kg body weight) (Novo Nordisk).

Insulin signaling. Mice were placed in conditions of insulin tolerance test. WAT, liver, and muscle were collected 10 min after insulin injection. Insulin-stimulated phosphorylation of Akt on Ser473 was analyzed by immunoblotting. Signals were quantified with Quantity One software (Bio-Rad).

Quantification of PGs in WAT. Quantification of $PGF_{2\alpha}$, PGE_2, and PGD_2 was performed on WAT from 5-week-old mice. Deuterated standards (10 ng of d4-$PGF_{2\alpha}$, d4-PGE_2, and d4-PGD_2 from Cayman Chemical) were added to homogenized tissue samples. Extraction and derivatization to obtain products of interest were performed as previously described (25). Quantification was performed after analysis of unlabeled and deuterated PGs by gas chromatography–mass spectrometry (Agilent Technologies).

Statistical analysis. Results are expressed as means ± SD. Statistical significance of differences between experimental groups was assessed using tests specified in figure legends.

RESULTS

Generation of *Akr1b7^−/−* mice. The strategy to generate *Akr1b7^−/−* mice is depicted in Fig. 1A–C. In WT mice, Akr1b7 was strongly detected in the adrenal gland and to a lesser extent in WAT. In contrast, it was undetectable in brown adipose tissue (BAT), muscle, or liver (Fig. 1D). Absence of Akr1b7 signal in KO tissues confirmed complete inactivation of the *Akr1b7* gene. Mouse also expresses two other members of Akr1b family, Akr1b3 and Akr1b8,
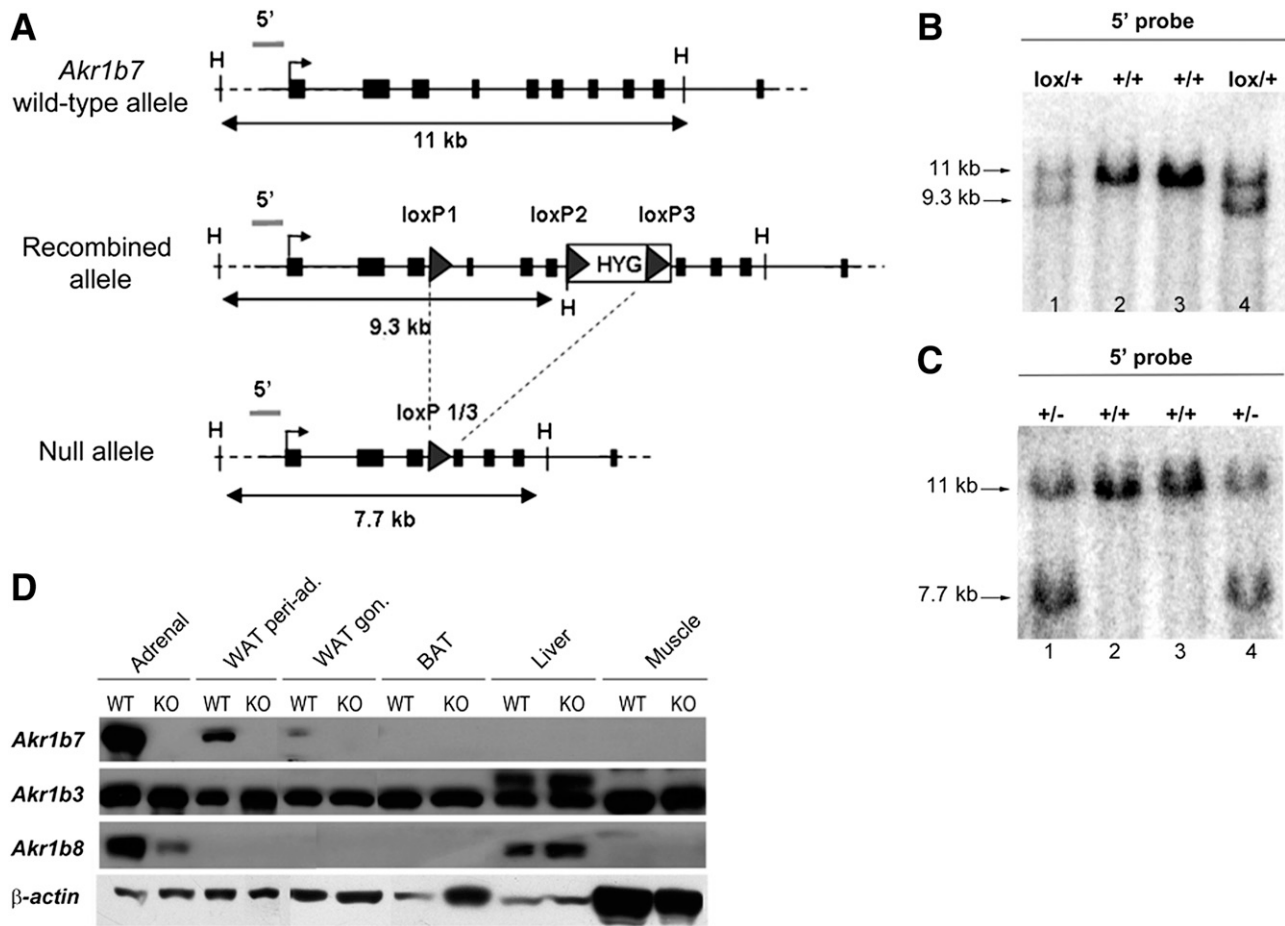
FIG. 1. Generation of *Akr1b7* KO mice. *A*: Genomic organization of the *Akr1b7* WT allele (*top*). *Akr1b7* exons are represented by black boxes. The 5′ probe used for the genotyping analyses is indicated by a gray bar. Genomic organization of the *Akr1b7* recombined allele (or triloxP conditional allele *Akr1b7^flox-hygro*) after homologous recombination of the targeting construct (*middle*). Genomic organization of the *Akr1b7*-null allele obtained after breeding of *Akr1b7^flox-hygro* homozygous females with MeuCre40 males (26) (*bottom*). Homologous recombination of the targeting construct and Cre-mediated recombination events between loxP1 and loxP3 sites, generating an *Akr1b7*-null allele, were screened by Southern blotting. *B*: Southern blot analysis of the homologous recombination of the targeting construct. The 5′ probe revealed an 11-kb *Hind*III (H in *A*) fragment corresponding to the WT allele and a 9.3-kb *Hind*III fragment corresponding to the recombined allele (*Akr1b7^flox-hygro*). *Lanes 2* and *3*: WT mice ($^{+/+}$). *Lanes 1* and *4*: heterozygous floxed mice (lox/+). *C*: Southern blot analysis for the *Akr1b7*-null allele. After Cre-mediated loxP recombination, mosaic animals containing the *Akr1b7*-null allele were crossed with WT animals to generate *Akr1b7^{+/−}* mice. The 5′ probe revealed a 7.7-kb *Hind*III fragment corresponding to the null allele. *Lanes 2* and *3*: WT mice ($^{+/+}$). *Lanes 1* and *4*: *Akr1b7^{+/−}* mice (+/−). *D*: Western blot analysis of Akr1b isoforms expression in different tissues from *Akr1b7^{+/+}* (WT) and *Akr1b7^{−/−}* (KO) mice. gon., gonadal; peri-ad., periadrenal.

but their expression pattern in adipose tissue has never been characterized. Using specific antibodies (25), we showed that Akr1b3 was expressed in all tissues tested, whereas Akr1b8 was absent from all adipose depots and muscle but abundant in adrenal and liver. Importantly, accumulation of both Akr1b3 and Akr1b8 isoforms was not upregulated in $Akr1b7^{−/−}$ tissues.

Akr1b7 ablation results in increased adipogenesis and lipogenesis. Under standard diet, $Akr1b7^{−/−}$ mice gained weight faster than WT mice starting at 7 to 8 weeks. This difference was exacerbated with time (Fig. 2*A*). Six-month-old $Akr1b7^{−/−}$ mice exhibited a significant excess of major WAT depots, such as gonadal, peri-adrenal, and inguinal WAT (Fig. 2*B*) and an increased liver mass. In contrast, weight of other organs including heart, kidney, and testis was not affected. Therefore, lack of Akr1b7 led to a significant overweight, correlated with expansion of WAT. This was confirmed by higher plasma leptin levels in KO mice (Table 1). In contrast, there was no alteration of adiponectin or resistin levels (Table 1).

Measurement of cross-sectional areas of adipocytes revealed clear adipocyte hypertrophy in all $Akr1b7^{−/−}$ white adipose depots compared with WT (Fig. 2*C*). In agreement with this observation, mRNA levels of the lipogenic genes *Scd1* and *Fasn* were found increased in mutant gonadal WAT (Fig. 2*D*), suggesting enhancement of the lipogenic capacity, although no change was recorded for expression of *Srebp-1c* and genes related to triglyceride synthesis. In addition, the DNA content of the fat depots was significantly higher in $Akr1b7^{−/−}$ than in WT mice, demonstrating increased cellularity (Fig. 2*E*). Altogether, these results suggest that under standard diet, deletion of *Akr1b7* leads to expansion of adipose tissue, which may be the result of improvement of both lipid storage, leading to adipocyte hypertrophy and adipogenesis, which leads to adipocyte hyperplasia.

The increased adiposity of $Akr1b7^{−/−}$ mice relative to their WT counterparts was not attributable to differences in food consumption and ambulatory activity. Indirect calorimetry revealed that $Akr1b7^{−/−}$ mice exhibited decreased energy expenditure (1.510 ± 0.055 vs. 1.358 ± 0.025 kJ/24 h/g)
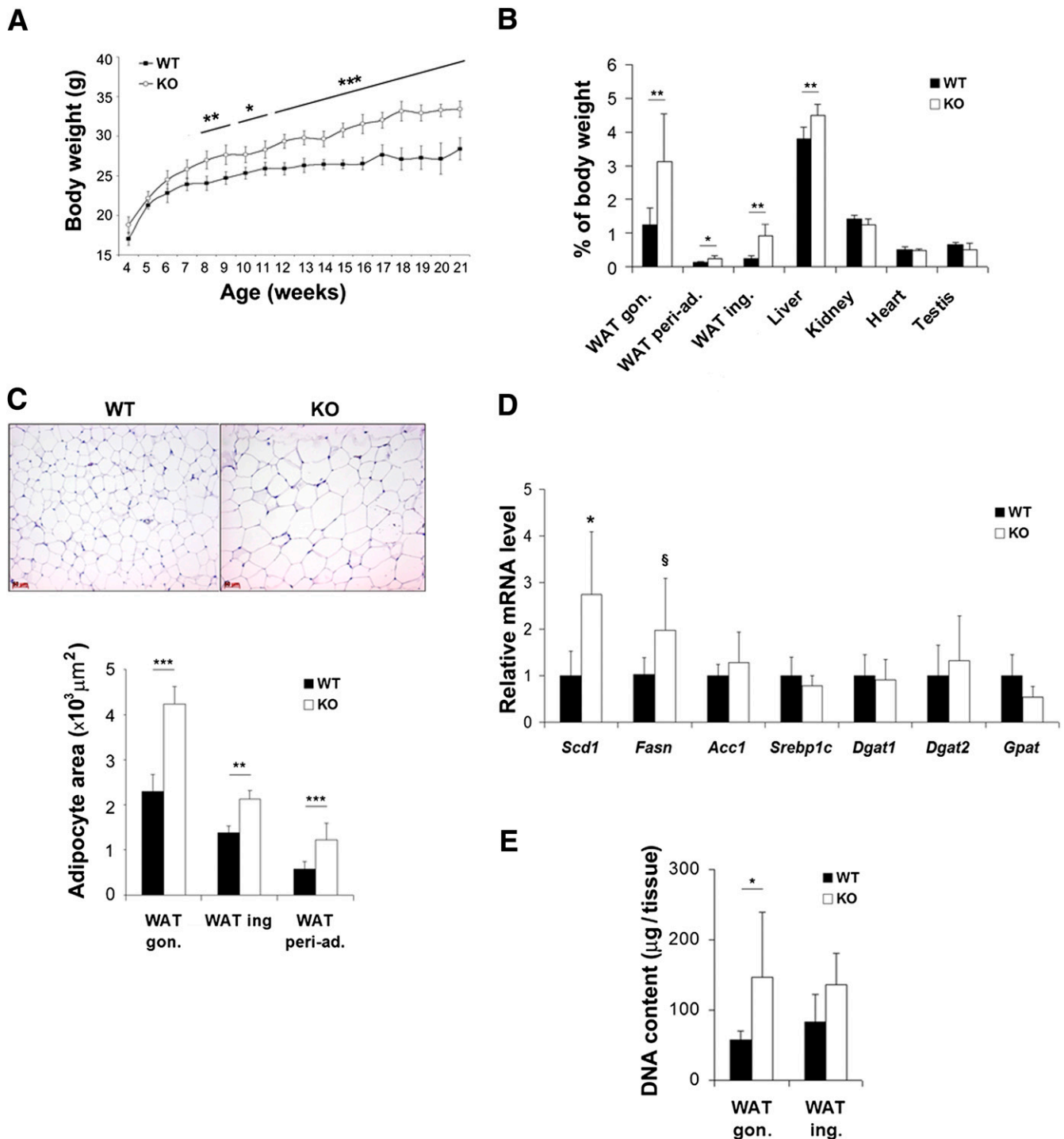
FIG. 2. Akr1b7 ablation leads to an excess of adipose tissue. *A*: Body weight of WT and *Akr1b7*$^{-/-}$ mice (KO) fed with a standard diet (*n* = 10–12/genotype). *P < 0.05, **P < 0.01, ***P < 0.001 using two-way ANOVA and Bonferroni posttest. *B*: Relative weight of major adipose tissue depots and other organs as a percentage of body weight from 6-month-old KO and WT mice (*n* = 6 to 7/group). *C*: Representative pictures showing microscopic hematoxylin/eosin-stained sections of gonadal adipose tissue (*top panel*) and area of adipocytes measured from paraffin sections of major adipose depots from 6-month-old KO and WT mice (*bottom panel*) (*n* = 4/group). *D*: *Scd1* is upregulated in WAT of *Akr1b7* null mice. *Scd1, Fasn, Acc1,* and *Srebp-1c* (lipogenesis) and *Dgat1, Dgat2,* and *Gpat* (triglyceride synthesis) gene expression were analyzed by RTqPCR on mRNAs from WAT of 6-month-old *Akr1b7* KO and WT mice. Bars represent the mean relative quantification (KO versus WT) of at least seven individual mice ± SD. *E*: Total DNA content in perigonadal and inguinal white fat pads from 6-month-old KO and WT mice (*n* = 7/group). gon., gonadal; ing, inguinal; peri-ad., periadrenal. *P < 0.05, **P < 0.01, ***P < 0.005, §P = 0.07 using Student *t* test. (A high-quality color representation of this figure is available in the online issue.)

and respiratory exchange ratio (0.91 ± 0.02 vs. 0.86 ± 0.02) (Supplementary Fig. 1). These data indicate that *Akr1b7*$^{-/-}$ mice have a lower metabolic rate and a switch to relatively more fat oxidation.

Lack of Akr1b7 predisposes to diet-induced obesity.
To test whether lack of *Akr1b7* gene could predispose to diet-induced obesity, we fed 5-week-old WT and KO mice with an HFD for 12 weeks and monitored growth.

TABLE 1
Plasma parameters of 24-week-old WT and *Akr1b7*-null mice

| Variables | Standard diet | | | | P value* |
	WT	n	*Akr1b7*$^{-/-}$	n	
Blood metabolites					
Triglycerides (g/L)	1.04 ± 0.1	14	1.07 ± 0.2	14	0.65
Cholesterol (g/L)	1.22 ± 0.2	14	1.18 ± 0.3	14	0.65
Free fatty acid (mmol/L)	0.93 ± 0.2	14	0.97 ± 0.3	14	0.73
Glycerol (μmol/L)	346 ± 62	14	365 ± 70	14	0.46
Glucocorticoid (ng/mL)	31.4 ± 17	5	37.1 ± 14	5	0.6
Adipokines					
Leptin (ng/mL)	6.70 ± 2.1	6	10.34 ± 2.3	6	0.04†
Adiponectin (ng/mL)	9.94 ± 2.3	6	11.11 ± 2.9	6	0.46
Resistin (ng/mL)	1.08 ± 0.1	6	1.15 ± 0.2	6	0.51

*P values are the results of nonpaired Student t test. †P ≤ 0.05.

In contrast with WT HFD mice, *Akr1b7*$^{-/-}$ HFD mice gained weight rapidly and became obese. This was associated with a fivefold increase in plasma leptin levels and reduced food intake (Fig. 3). The exacerbated obese phenotype observed in *Akr1b7*$^{-/-}$ mice fed with an HFD compared with regular diet was accompanied by a marked increase in plasma levels of triglycerides, glycerol, and free fatty acids, which remained unchanged under a standard diet (Tables 1 and 2). We concluded that lack of Akr1b7 predisposed mice to develop severe obesity on an HFD.

***Akr1b7*$^{-/-}$ mice display liver steatosis and progressive insulin resistance.** Oil Red O staining and triglycerides assays revealed that *Akr1b7*$^{-/-}$ liver accumulated a large amount of lipid droplets and contained twice as many triglycerides than WT (Supplementary Fig. 2A), confirming that *Akr1b7*$^{-/-}$ mice fed with a standard diet developed liver steatosis from 6 months of age.

To determine the respective roles of WAT lipolysis and liver lipogenesis in steatosis, plasmatic pools of lipids were measured, and mRNAs of genes involved in lipid and glucose metabolism were quantified in the liver. Compared with WT mice, *Akr1b7*$^{-/-}$ mice showed unchanged fasted plasma levels of free fatty acids and glycerol (Table 1), suggesting that lack of Akr1b7 did not increase basal WAT lipolysis. In contrast, the significant increase in *Scd1*

expression in the liver of KO mice was correlated to the presence of steatosis (Supplementary Fig. 2B). However, this link remains unclear because expression of upstream lipogenic genes and triglyceride synthesis genes was unchanged. Finally, mRNA expression of genes related to β-oxidation and gluconeogenesis was unaltered in mutant mice.

Excess of adipose tissue and liver steatosis are frequently associated with altered glucose homeostasis and insulin resistance. Although fasting plasma glucose tended to be more elevated in 6-month-old *Akr1b7*$^{-/-}$ than in WT mice (Fig. 4A, *right*), both exhibited similar responses to the glucose tolerance test (Fig. 4A, *left*). However, *Akr1b7*$^{-/-}$ mice showed an attenuated response to insulin during the insulin tolerance test (Fig. 4B, *left*). The absence of significant fasted hyperglycemia in *Akr1b7*$^{-/-}$ mice along with basal hyperinsulinemia (Fig. 4B, *right*) suggest a resistance to the insulin-mediated action on hepatic glucose output.

To examine time-dependent changes in insulin sensitivity, we quantified Akt phosphorylation on Ser473 in response to insulin surge in peripheral tissues of 3-, 6-, and 9-month-old mutant and WT mice. Insulin-induced Akt phosphorylation remained unchanged in muscle, liver, or WAT of 3-month-old *Akr1b7*$^{-/-}$ mice (Fig. 4C) in agreement with their normal response to the insulin tolerance
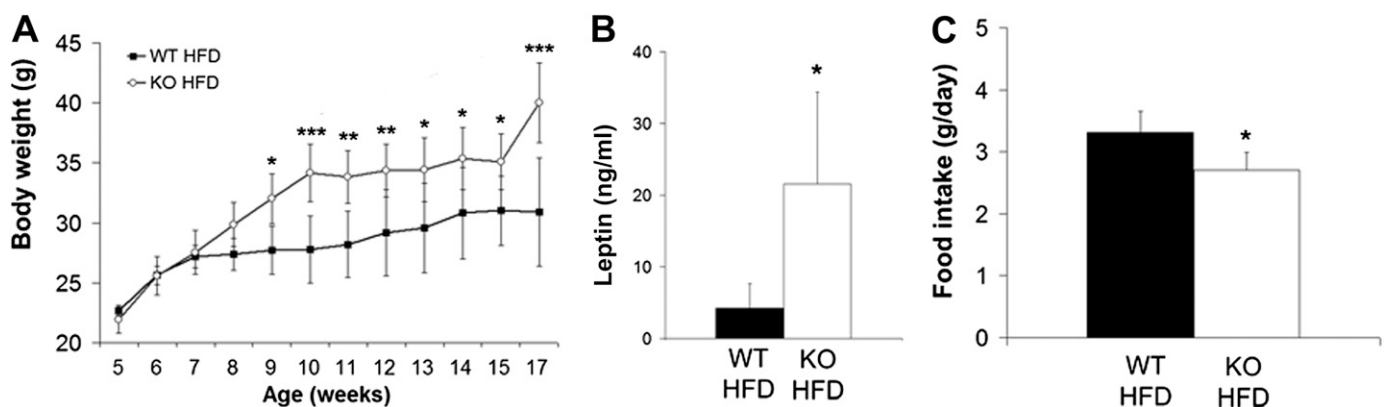

FIG. 3. *Akr1b7*$^{-/-}$ mice are more sensitive to diet-induced obesity. A: Body weight gain of WT and *Akr1b7*$^{-/-}$ mice fed with HFD. *P < 0.05, **P < 0.01, ***P < 0.001 using two-way ANOVA and Bonferroni posttest. B: Plasma leptin levels of 17-week-old WT and *Akr1b7*$^{-/-}$ mice fed with HFD. C: Food intake measured at 16 weeks of age every day over a 6-day period during HFD. n = 6 to 7/group for each experiment. *P < 0.05 using Student t test.

TABLE 2
Plasma parameters of 17-week-old WT and *Akr1b7*-null mice fed with a high-fat diet for 12 weeks

| | High-fat diet | | | | |
Variables	WT	n	$Akr1b7^{-/-}$	n	P value*
Blood metabolites					
Triglycerides (g/L)	0.83 ± 0.12	7	1.2 ± 0.24	6	0.01†
Cholesterol (g/L)	1.45 ± 0.33	7	1.41 ± 0.24	6	0.79
Free fatty acid (mmol/L)	0.63 ± 0.11	7	0.75 ± 0.10	6	0.06
Glycerol (µmol/L)	276 ± 58	7	427 ± 94	6	0.009†
Adipokines					
Leptin (ng/mL)	4.22 ± 3.37	7	21.6 ± 12.8	6	0.03‡
Adiponectin (ng/mL)	9.31 ± 2.56	6	15.12 ± 2.33	6	0.02‡
Resistin (ng/mL)	2.09 ± 1.0	6	1.50 ± 0.61	6	0.25

*P values are the results of nonpaired Student t test. †$P \leq 0.01$, ‡$P \leq 0.05$.

test (not shown). In contrast, insulin-dependent Ser473 phosphorylation was reduced by 42% in liver from mutant mice of 6 months of age, whereas both muscle and WAT retained normal insulin response. Finally, Akt phosphorylation was reduced by at least 40% in all three tissues from 9-month-old mutant mice (Fig. 4C). Thus, whole-body insulin resistance observed in mutant mice of 6 months of age is at least linked to a defect in insulin-induced Akt phosphorylation in liver. In these mice, unaffected insulin responsiveness in other peripheral tissues implies normal muscle (and WAT) glucose disposal and likely explains the unaffected postchallenge glucose levels (Fig. 4A). Importantly, progressive insulin resistance of $Akr1b7^{-/-}$ mice occurs from the age of 6 months secondarily to establishment of the overweight phenotype.

Expansion of $Akr1b7^{-/-}$ adipose tissue is linked to decreased PGF$_{2\alpha}$ levels. Our observations suggest that Akr1b7 is acting on adipose tissue by regulating both adipocyte differentiation and lipogenesis. We previously showed that Akr1b7 is endowed with a PGFS activity both in vitro and in living cells (17,25). When we compared the levels of various PGs in adipose tissue from $Akr1b7^{-/-}$ and WT mice (Fig. 5A), we found that PGF$_{2\alpha}$ contents were specifically reduced by 45% in Akr1b7-deficient adipose tissue, whereas PGE$_2$ and PGD$_2$ were unaltered. Importantly, these changes occurred without any alteration in *Akr1b3* gene expression (Fig. 5B), which has been reported to affect adipocyte differentiation in vitro (18). We next examined expression of the receptors for PGF$_{2\alpha}$ (FP$_A$ and FP$_B$) in various mouse tissues and found that adipose depots were major sites of FP protein expression (Fig. 5C).

To confirm that the alteration of adipose tissue homeostasis resulted from decreased PGF$_{2\alpha}$ production, 4-week-old $Akr1b7^{-/-}$ mice were treated daily for 3 months with cloprostenol, a synthetic PGF$_{2\alpha}$. Plasma leptin levels of $Akr1b7^{-/-}$ mice were significantly decreased by cloprostenol (Fig. 6A), reflecting a reduction of WAT mass. Indeed, compared with $Akr1b7^{-/-}$ control mice, mice injected with cloprostenol showed a significant reduction in adipocyte areas and lower *Scd1* gene expression in gonadal WAT (Fig. 6B and C). Hence, in good agreement with the PGFS activity of Akr1b7, cloprostenol treatment was able to correct increased adiposity observed in Akr1b7-deficient mice.

Our in vivo data (Figs. 2C–E and 6A–C) showed that lack of Akr1b7, by lowering PGF$_{2\alpha}$ levels, led to hypertrophy of adipocytes in which high levels of FP receptors were detected (Fig. 5C). To test a direct impact of PGF$_{2\alpha}$ on

lipogenesis, we treated 3T3-L1 adipocytes with various concentrations of cloprostenol. Cloprostenol reduced mRNA levels of *Scd1* and *Fasn* genes in a dose-dependent manner, whereas neither *Srebp-1c* transcripts nor mature protein levels were affected (Fig. 6D). This result demonstrated that in addition to inhibiting adipocyte differentiation, PGF$_{2\alpha}$ could also repress lipogenic genes in mature adipocytes in an Srebp-1c–independent manner.

To test the possibility that expansion of WAT in $Akr1b7^{-/-}$ mice could also be the result of an improved recruitment of new adipocytes, mice were exposed to HFD for 5 weeks in the presence or absence of cloprostenol and treated with BrdU for the last 3 weeks. In agreement with the sensitivity of Akr1b7-deficient WAT to expand in response to long-term HFD (Fig. 3), a 5-week exposure to HFD was sufficient to impart a 7.7-fold increase of gonadal WAT mass in $Akr1b7^{-/-}$ mice compared with the 1.7-fold increase observed in WT mice (Fig. 6E). Concomitant cloprostenol treatment eventually reduced the expansion of mutant WAT mass to values similar to those of mutant mice fed with a standard diet. Quantification of new adipocyte production during HFD exposure revealed a 3.5-fold increase in BrdU-positive adipocyte-associated nuclei in gonadal WAT from $Akr1b7^{-/-}$ compared with WT mice (Fig. 6F). Cloprostenol treatment of $Akr1b7^{-/-}$ mice reduced production of new adipocytes during HFD-induced adipose tissue expansion to values similar to those of WT mice fed with HFD. Altogether, these data supported in vivo evidence that the PGFS activity of Akr1b7 regulates adipose tissue expansion by repressing both adipocyte hypertrophy and adipocyte recruitment.

DISCUSSION

Akr1b7 has antiadipogenic and antilipogenic activities. We investigated the physiological function of Akr1b7, a protein enriched in stromal vascular fraction of WAT, by generating a KO mouse model. Our results showed for the first time the direct contribution of a protein producing the antiadipogenic paracrine factor PGF$_{2\alpha}$ in the regulation of adipose tissue expansion. Indeed, even under standard diet, $Akr1b7^{-/-}$ mice exhibited an increased number and size of white adipose cells. This increased adiposity was correlated with a specific decrease in PGF$_{2\alpha}$ concentrations in WAT. The ability of chronic administration of a PGF$_{2\alpha}$ agonist to reverse the adipose phenotype of $Akr1b7^{-/-}$ mice shows that antiadipogenic activity of Akr1b7 is essentially resulting from its PGFS activity.
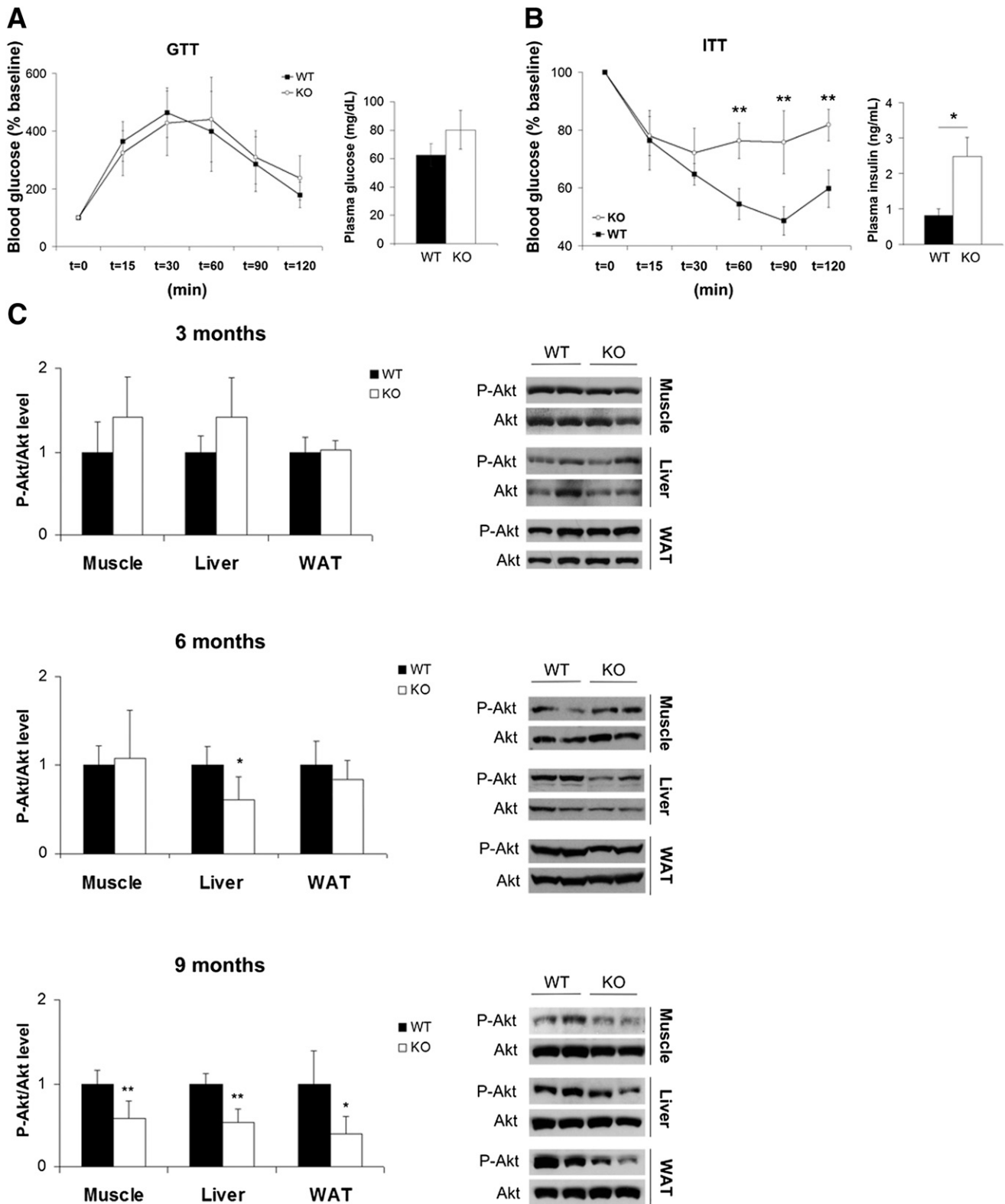
FIG. 4. Lack of Akr1b7 leads to insulin resistance. *A* and *B*: *Left*, glucose tolerance test (GTT) and insulin tolerance test (ITT). Six-month-old WT and *Akr1b7* null mice (*n* = 7/group) were either fasted for 16 h before receiving an intraperitoneal injection of 2 g/kg glucose or 5 h before receiving an intraperitoneal injection of 0.75 units/kg insulin. Blood glucose concentration was measured at the indicated time points. *Right*, fasting plasma glucose and insulin levels of the WT and *Akr1b7* KO mice fasted overnight. *C*: *Right*, Western blot analysis of phospho-Akt (P-Akt) at Ser473 and total Akt levels in WAT, liver, and muscle of 3- (*top*), 6- (*middle*), and 9-month-old (*bottom*) WT and *Akr1b7* KO mice after insulin injection. *Left*, quantifications of insulin-induced Akt Ser473 phosphorylation reported to total Akt levels in WT and *Akr1b7* KO mice normalized with β-actin signal. *P < 0.05, **P < 0.005 using Student *t* test.
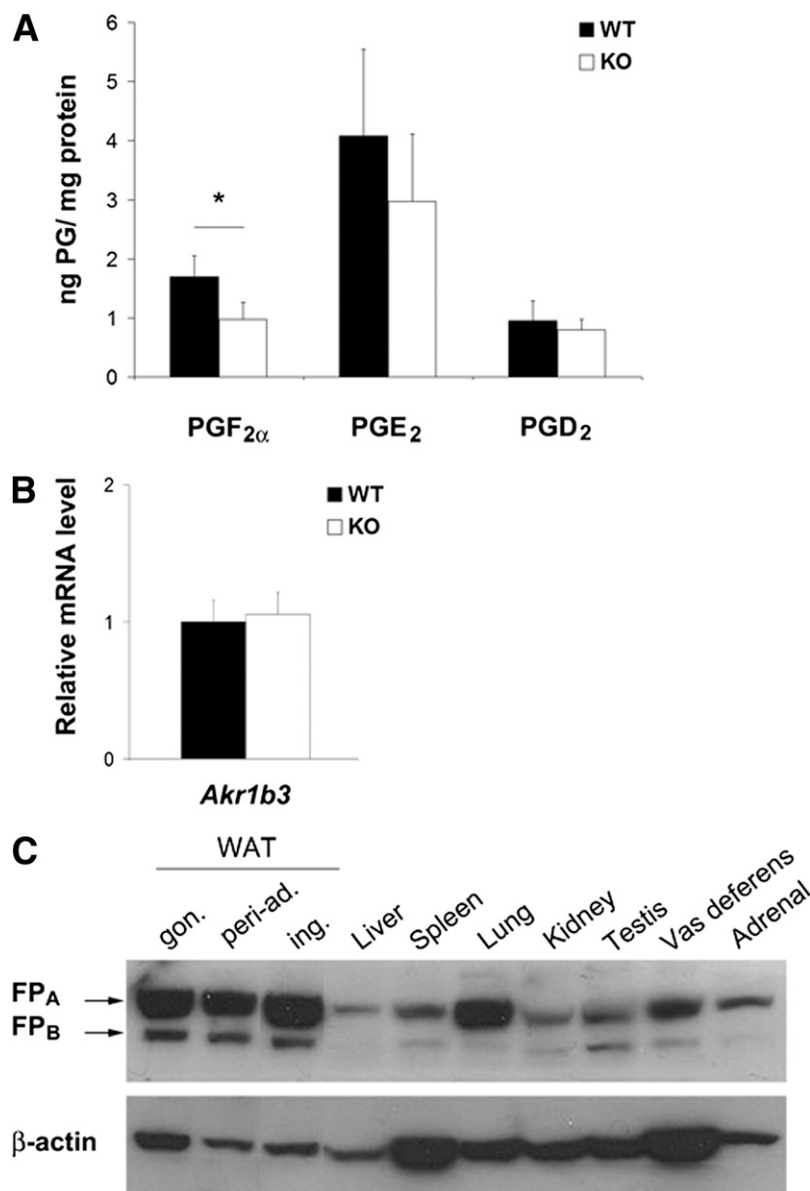
FIG. 5. Decreased levels of PGF$_{2\alpha}$ in *Akr1b7*$^{-/-}$ adipose tissue. *A*: PG contents measured by mass spectrometry of adipose tissue from 5-week-old WT and *Akr1b7* KO mice. *B*: Relative mRNA levels of *Akr1b3* in WAT of WT and KO mice (n = 6/group). *C*: Western blot analysis of FP receptor isoforms expression in different tissues from WT mice. gon., gonadal; ing., inguinal; peri-ad., periadrenal. *$P < 0.05$ using Student t test.

This is the first demonstration that PGF$_{2\alpha}$ is indeed an antiadipogenic molecule in vivo. Moreover, we showed that the antiadipogenic function of PGF$_{2\alpha}$ was not only resulting from inhibition of the recruitment of preadipocytes but also from inhibition of adipocyte lipogenesis in *Akr1b7*$^{-/-}$ mice. This direct effect of PGF$_{2\alpha}$ on lipogenesis was confirmed in 3T3-L1 adipocytes.

Akr1b7$^{-/-}$ mice showed exacerbated sensitivity to obesity in a 129/Sv genetic background. This phenotype is associated with metabolic disorders such as hepatosteatosis and insulin resistance even under standard diet. Therefore, *Akr1b7*$^{-/-}$ mouse is a powerful model to study obesity and its complications.

The phenotype of *Akr1b7*$^{-/-}$ mice is linked to Akr1b7 function in adipose tissue. In the adrenal cortex, *Akr1b7* expression was shown to limit glucocorticoids release under stress conditions through an internal-feedback loop (25). Glucocorticoids are powerful regulators of adipose tissue homeostasis (30). Nevertheless, we showed that basal plasma corticosterone levels were not affected in *Akr1b7*$^{-/-}$ mice (Table 1). This excludes an adrenal contribution to the adipose phenotype.

In the intestine, *Akr1b7* expression is regulated by several nuclear receptors and is mainly implicated in detoxification processes by metabolizing bile acids or lipid peroxidation products (23,31,32). This function could influence nutrient intake and disrupt energy balance. However, we did not find any alterations of food consumption, fecal production, or fat content (Supplementary Fig. 1) and intestine histology (not shown) in *Akr1b7*$^{-/-}$ mice. Therefore, it seems unlikely that lack of Akr1b7 in the intestine could account for increased adiposity in *Akr1b7*$^{-/-}$ mice.

Akr1b14 mRNA, the rat ortholog of *Akr1b7*, is undetectable in the liver until induction by growth hormone
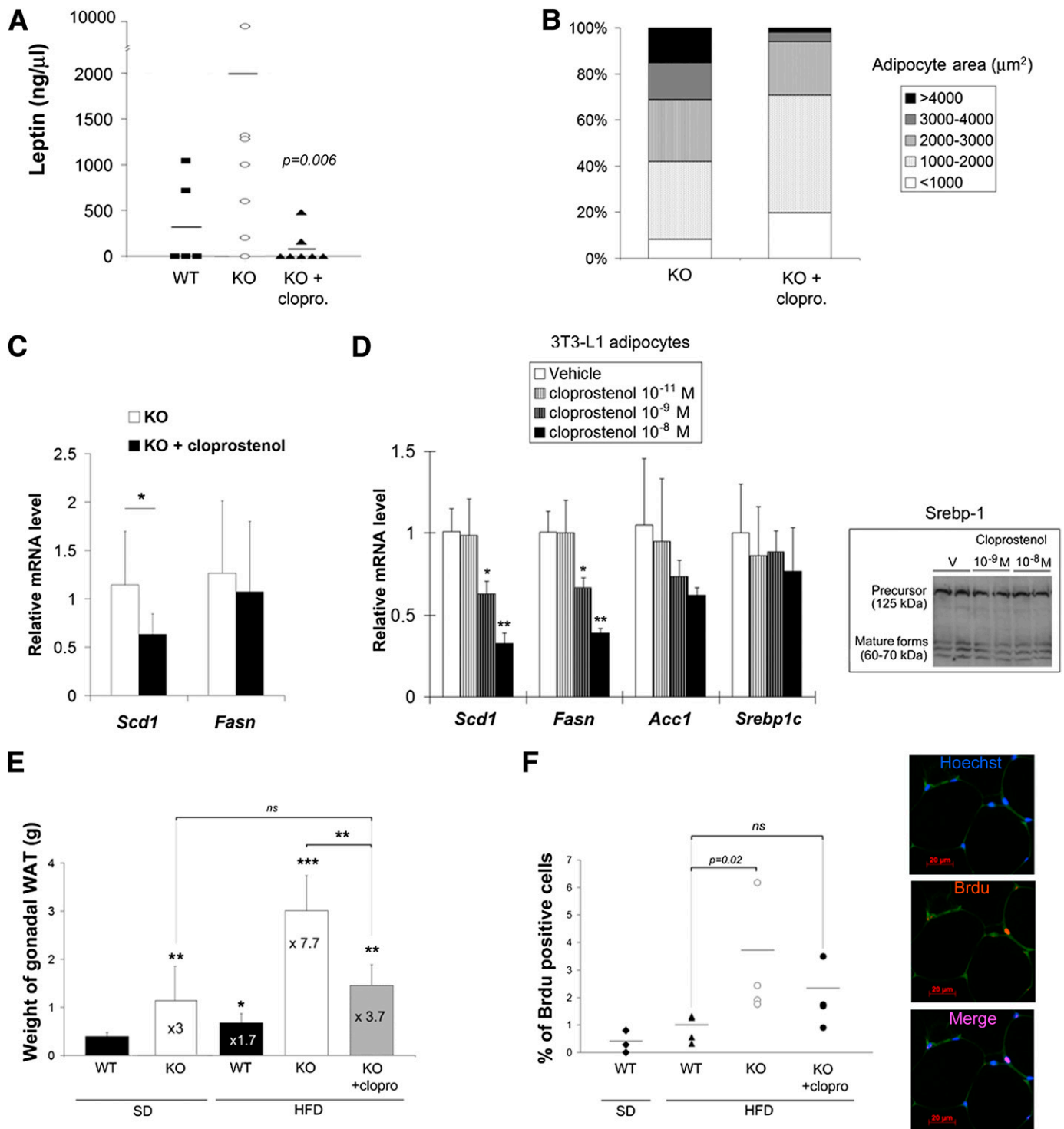
FIG. 6. Phenotypic rescue by injection of PGF$_{2\alpha}$ agonist. A–C: *Akr1b7*-null mice were daily injected with 0.1 µg/g body weight of cloprostenol, a PGF$_{2\alpha}$ agonist, or with vehicle from 4–16 weeks of age (*n* = 7–9/group). A: Fasted plasma leptin levels from vehicle WT and KO mice and from KO mice treated with cloprostenol (KO + clopro.); statistical significance was assessed by Mann–Whitney test. B: Representation of adipocyte proportion according to their size. Adipocyte area was measured on paraffin sections from *Akr1b7* KO mice treated with vehicle (KO) or with cloprostenol (KO + clopro.). C: Expression of lipogenic genes *Scd1* and *Fasn* in adipose tissue from *Akr1b7* KO mice treated with vehicle (KO) or with cloprostenol (KO + cloprostenol) analyzed by RTqPCR. D: RTqPCR of lipogenic genes *Scd1*, *Fasn*, *Acc1*, and *Srebp-1c* (*left*) and Western blot analysis of Srebp-1 precursor and mature cleaved forms in 3T3-L1 adipocytes (*right*). Differentiated adipocytes were treated 24 h with various concentrations of cloprostenol or with vehicle. E and F: Cloprostenol effect on adipose tissue expansion induced by 5-week HFD in *Akr1b7* KO mice. E: Weight of gonadal WAT from WT mice, KO mice, and KO mice treated with cloprostenol (KO+clopro) after standard diet (SD) or HFD. F: Detection of new adipocyte production in vivo by BrdU labeling. Confocal immunofluorescence analysis was performed on paraffin section taken from WT and KO animals exposed to BrdU over the last 3 weeks of the 5-week HFD with or without cloprostenol treatment. Nuclei were stained using Hoechst, and autofluorescence from the green channel was used to detect tissue structures. Quantification of BrdU-positive adipocyte-associated nuclei was carried out from *n* = >900 nuclei/group (*n* = 4/group). *$P < 0.05$, **$P < 0.01$, ***$P < 0.005$ using Student *t* test. (A high-quality digital representation of this figure is available in the online issue.)

or oxidative stress (33,34). In mouse, *Akr1b7* expression is hardly detected in the liver under basal conditions (21) but is inducible by farnesoid X receptor/pregnane X receptor agonists (31,32). Recently, it was shown that forced over-expression of Akr1b7 in the liver using adenoviral vector significantly lowered hepatic lipid contents in genetically obese mice, suggesting a protective effect against hepatosteatosis (35). Hence, we cannot completely exclude that hepatosteatosis observed in *Akr1b7*$^{-/-}$ mice could also result from the chronic lack of a very faint hepatic expression of the enzyme. However, several arguments suggest that this metabolic complication is rather the consequence of altered adipose tissue physiology in *Akr1b7*-null mice. First, using our antibody designed to discriminate Akr1b isoforms (25,36), we never managed to detect Akr1b7 in WT mouse liver (Fig. 1*D*). Second, we demonstrated that hepatosteatosis and insulin resistance were established from the age of 6 months, far after the increase of adiposity in *Akr1b7*$^{-/-}$ mice. Finally, it is well-established that excessive development of adipose tissue can lead to hepatosteatosis and insulin resistance through several interconnected pathways (37). Thus, the overall phenotype of *Akr1b7*$^{-/-}$ mice can mainly be attributed to Akr1b7 function in the adipose tissue.

Akr1b7-null mice phenotype does not rely on defects in detoxification of lipid peroxidation by-products. Besides its PGF$_{2\alpha}$ synthase activity, Akr1b7 has other reported enzymatic activities with possible impacts on adipose tissue, such as reduction of 4-hydroxynonenal (4-HNE) (17,25,38). Increased 4-HNE levels in response to oxidative stress promote and perpetuate the obese state (39) and can be involved in the development of insulin resistance (40,41). Oxidative stress in human and murine adipose tissue as well as in 3T3-L1 adipocytes affects the secretion of adipokines such as adiponectin and proinflammatory cytokines (1,41,42). However, *Akr1b7*$^{-/-}$ mice showed no change in adiponectin levels (Table 1) and no significant increase of macrophage infiltration before the age of 6 months (Supplementary Fig. 3). This indicates that excess adiposity of *Akr1b7*$^{-/-}$ mice preceded elevation of inflammatory status. Moreover, we observed similar amounts of 4-HNE–protein adducts in liver, muscle, and adipose tissue from WT and mutant mice (Supplementary Fig. 4). These results indicate that increased adiposity and insulin resistance in mutant mice is not linked to alteration of intracellular 4-HNE detoxification.

Akr1b7-dependent production of PGF$_{2\alpha}$ regulates adipose tissue homeostasis. For decades, PGF$_{2\alpha}$ has been implicated in the inhibition of adipogenesis (12–14), but its function on adipocyte differentiation was never established in vivo or tested on already differentiated tissues. We demonstrate in this study that a decrease in intra-adipose tissue PGF$_{2\alpha}$ levels following Akr1b7 ablation leads to increased adiposity. This phenotype results from alleviation of the repression exerted on both adipocyte precursors recruitment and on lipid storage in mature adipocytes and can be reverted by exogenous PGF$_{2\alpha}$ injections. Using 3T3-L1 adipocytes, we confirmed that PGF$_{2\alpha}$ inhibited expression of lipogenic enzymes. This unsuspected result is consistent with the high expression of the FP receptor in cultured adipocytes (18) and in vivo (Fig. 5*C*). The mechanism leading to PGF$_{2\alpha}$-mediated inhibition of lipogenic genes remains to be explored. We showed in this paper that it occurs independently of Srebp-1c, in agreement with previous findings indicating that Srebp-1c does not transactivate lipogenic genes in adipocytes (43).

Akr1b family members: novel actors in adipose tissue homeostasis? In mouse, aldose reductases Akr1b3 and Akr1b7 are so far the only members of the Akr1b family that are expressed in adipose tissue (Fig. 1*D*). A recent study indicated that PGFS activity of Akr1b3 could influence adipogenesis. Indeed, siRNA-mediated Akr1b3 knockdown decreased the concentrations of PGF$_{2\alpha}$ in 3T3-L1 medium, which resulted in enhanced adipogenesis (18). The presence of Akr1b3 could thus account for maintenance of a low level of PGF$_{2\alpha}$ in the adipose tissue of *Akr1b7*$^{-/-}$ mice (Fig. 5*A*). However, this isoform was not able to compensate for the lack of Akr1b7. Moreover, no defect in adipose tissue homeostasis was reported in *Akr1b3*$^{-/-}$ mice but careful in vivo investigations will be needed to definitively conclude (19).

Among human members of the AKR family, AKR1B1 and AKR1C3 exhibited a PG synthase activity in vitro. AKR1C3 is expressed in human adipocytes and was for a long time considered as the only PGFS in humans (44,45). However, AKR1B1 was recently shown to have a higher PGFS activity than AKR1C3 in vitro (17) and to be highly active in human endometrium (46). The role of AKR1B1 has been extensively studied in the pathogenesis of diabetes complications (47), but its role in the physiology of adipose tissue is an almost virgin field of investigation. One could hypothesize that AKR1B1 could act as an antiadipogenic factor through local PGF$_{2\alpha}$ production.

In conclusion, our mouse model provides functional evidence for novel mechanisms linking prostanoid metabolism with adipose tissue homeostasis. It also opens up new perspectives on the potential contribution of AKR1B isoforms to physiological control of adipose tissue expansion and pathogenesis of obesity in patients.

REFERENCES

1. Haslam DW, James WP. Obesity. Lancet 2005;366:1197–1209
2. Knittle JL, Timmers K, Ginsberg-Fellner F, Brown RE, Katz DP. The growth of adipose tissue in children and adolescents. Cross-sectional and longitudinal studies of adipose cell number and size. J Clin Invest 1979;63:239–246
3. Spalding KL, Arner E, Westermark PO, et al. Dynamics of fat cell turnover in humans. Nature 2008;453:783–787
4. Kershaw EE, Flier JS. Adipose tissue as an endocrine organ. J Clin Endocrinol Metab 2004;89:2548–2556
5. Rosen ED, MacDougald OA. Adipocyte differentiation from the inside out. Nat Rev Mol Cell Biol 2006;7:885–896
6. Rosen ED, Spiegelman BM. Adipocytes as regulators of energy balance and glucose homeostasis. Nature 2006;444:847–853
7. Otto TC, Lane MD. Adipose development: from stem cell to adipocyte. Crit Rev Biochem Mol Biol 2005;40:229–242
8. Rosen ED, Spiegelman BM. Molecular regulation of adipogenesis. Annu Rev Cell Dev Biol 2000;16:145–171
9. Fujitani Y, Aritake K, Kanaoka Y, et al. Pronounced adipogenesis and increased insulin sensitivity caused by overproduction of prostaglandin D2 in vivo. FEBS J 2010;277:1410–1419
10. Ghoshal S, Trivedi DB, Graf GA, Loftin CD. Cyclooxygenase-2 deficiency attenuates adipose tissue differentiation and inflammation in mice. J Biol Chem 2011;286:889–898
11. Jaworski K, Ahmadian M, Duncan RE, et al. AdPLA ablation increases lipolysis and prevents obesity induced by high-fat feeding or leptin deficiency. Nat Med 2009;15:159–168
12. Casimir DA, Miller CW, Ntambi JM. Preadipocyte differentiation blocked by prostaglandin stimulation of prostanoid FP2 receptor in murine 3T3-L1 cells. Differentiation 1996;60:203–210
13. Serrero G, Lepak NM. Prostaglandin F2alpha receptor (FP receptor) agonists are potent adipose differentiation inhibitors for primary culture of adipocyte precursors in defined medium. Biochem Biophys Res Commun 1997;233:200–202
14. Fujimori K, Ueno T, Amano F. Prostaglandin F(2alpha) suppresses early phase of adipogenesis, but is not associated with osteoblastogenesis in mouse mesenchymal stem cells. Prostaglandins Other Lipid Mediat 2010;93:52–59
15. Liu L, Clipstone NA. Prostaglandin F2alpha inhibits adipocyte differentiation via a G alpha q-calcium-calcineurin-dependent signaling pathway. J Cell Biochem 2007;100:161–173
16. Liu L, Clipstone NA. Prostaglandin F2alpha induces the normoxic activation of the hypoxia-inducible factor-1 transcription factor in differentiating 3T3-L1 preadipocytes: Potential role in the regulation of adipogenesis. J Cell Biochem 2008;105:89–98
17. Kabututu Z, Manin M, Pointud J-C, et al. Prostaglandin F2alpha synthase activities of aldo-keto reductase 1B1, 1B3 and 1B7. J Biochem 2009;145:161–168
18. Fujimori K, Ueno T, Nagata N, et al. Suppression of adipocyte differentiation by aldo-keto reductase 1B3 acting as prostaglandin F2alpha synthase. J Biol Chem 2010;285:8880–8886
19. Baba SP, Hellmann J, Srivastava S, Bhatnagar A. Aldose reductase (AKR1B3) regulates the accumulation of advanced glycosylation end products (AGEs) and the expression of AGE receptor (RAGE). Chem Biol Interact 2011;191:357–363
20. Brockstedt E, Peters-Kottig M, Badock V, Hegele-Hartung C, Lessl M. Luteinizing hormone induces mouse vas deferens protein expression in the murine ovary. Endocrinology 2000;141:2574–2581
21. Lau ET, Cao D, Lin C, Chung SK, Chung SS. Tissue-specific expression of two aldose reductase-like genes in mice: abundant expression of mouse vas deferens protein and fibroblast growth factor-regulated protein in the adrenal gland. Biochem J 1995;312:609–615
22. Martinez A, Aigueperse C, Val P, et al. Physiological functions and hormonal regulation of mouse vas deferens protein (AKR1B7) in steroidogenic tissues. Chem Biol Interact 2001;130-132:903–917
23. Volle DH, Repa JJ, Mazur A, et al. Regulation of the aldo-keto reductase gene akr1b7 by the nuclear oxysterol receptor LXRalpha (liver X receptor-alpha)
24. in the mouse intestine: putative role of LXRs in lipid detoxification processes. Mol Endocrinol 2004;18:888–898
24. Tirard J, Gout J, Lefrançois-Martinez AM, Martinez A, Begeot M, Naville D. A novel inhibitory protein in adipose tissue, the aldo-keto reductase AKR1B7: its role in adipogenesis. Endocrinology 2007;148:1996–2005
25. Lambert-Langlais S, Pointud J-C, Lefrançois-Martinez A-M, et al. Aldo keto reductase 1B7 and prostaglandin F2alpha are regulators of adrenal endocrine functions. PLoS ONE 2009;4:e7309
26. Leneuve P, Colnot S, Hamard G, et al. Cre-mediated germline mosaicism: a new transgenic mouse for the selective removal of residual markers from tri-lox conditional alleles. Nucleic Acids Res 2003;31:e21
27. Baumann C, Davies B, Peters M, Kaufmann-Reiche U, Lessl M, Theuring F. AKR1B7 (mouse vas deferens protein) is dispensable for mouse development and reproductive success. Reproduction 2007;134:97–109
28. Weir JB. New methods for calculating metabolic rate with special reference to protein metabolism. J Physiol 1949;109:1–9
29. Grizard G, Sion B, Bauchart D, Boucher D. Separation and quantification of cholesterol and major phospholipid classes in human semen by high-performance liquid chromatography and light-scattering detection. J Chromatogr B Biomed Sci Appl 2000;740:101–107
30. Masuzaki H, Paterson J, Shinyama H, et al. A transgenic model of visceral obesity and the metabolic syndrome. Science 2001;294:2166–2170
31. Liu MJ, Takahashi Y, Wada T, et al. The aldo-keto reductase Akr1b7 gene is a common transcriptional target of xenobiotic receptors pregnane X receptor and constitutive androstane receptor. Mol Pharmacol 2009;76:604–611
32. Schmidt DR, Schmidt S, Holmstrom SR, et al. AKR1B7 is induced by the farnesoid X receptor and metabolizes bile acids. J Biol Chem 2011;286:2425–2432
33. Kotokorpi P, Gardmo C, Nyström CS, Mode A. Activation of the glucocorticoid receptor or liver X receptors interferes with growth hormone-induced akr1b7 gene expression in rat hepatocytes. Endocrinology 2004;145:5704–5713
34. Jia G, Takahashi R, Zhang Z, Tsuji Y, Sone H. Aldo-keto reductase 1 family B7 is the gene induced in response to oxidative stress in the livers of Long-Evans Cinnamon rats. Int J Oncol 2006;29:829–838
35. Ge X, Yin L, Ma H, Li T, Chiang JY, Zhang Y. Aldo-keto reductase 1B7 is a target gene of FXR and regulates lipid and glucose homeostasis. J Lipid Res 2011;52:1561–1568
36. Lefrançois-Martinez A-M, Bertherat J, Val P, et al. Decreased expression of cyclic adenosine monophosphate-regulated aldose reductase (AKR1B1) is associated with malignancy in human sporadic adrenocortical tumors. J Clin Endocrinol Metab 2004;89:3010–3019
37. Qatanani M, Lazar MA. Mechanisms of obesity-associated insulin resistance: many choices on the menu. Genes Dev 2007;21:1443–1455
38. Lefrançois-Martinez AM, Tournaire C, Martinez A, et al. Product of side-chain cleavage of cholesterol, isocaproaldehyde, is an endogenous specific substrate of mouse vas deferens protein, an aldose reductase-like protein in adrenocortical cells. J Biol Chem 1999;274:32875–32880
39. Singh SP, Niemczyk M, Saini D, Awasthi YC, Zimniak L, Zimniak P. Role of the electrophilic lipid peroxidation product 4-hydroxynonenal in the development and maintenance of obesity in mice. Biochemistry 2008;47:3900–3911
40. Grimsrud PA, Picklo MJ Sr, Griffin TJ, Bernlohr DA. Carbonylation of adipose proteins in obesity and insulin resistance: identification of adipocyte fatty acid-binding protein as a cellular target of 4-hydroxynonenal. Mol Cell Proteomics 2007;6:624–637
41. Soares AF, Guichardant M, Cozzone D, et al. Effects of oxidative stress on adiponectin secretion and lactate production in 3T3-L1 adipocytes. Free Radic Biol Med 2005;38:882–889
42. Furukawa S, Fujita T, Shimabukuro M, et al. Increased oxidative stress in obesity and its impact on metabolic syndrome. J Clin Invest 2004;114:1752–1761
43. Sekiya M, Yahagi N, Matsuzaka T, et al. SREBP-1-independent regulation of lipogenic gene expression in adipocytes. J Lipid Res 2007;48:1581–1591
44. Quinkler M, Bujalska IJ, Tomlinson JW, Smith DM, Stewart PM. Depot-specific prostaglandin synthesis in human adipose tissue: a novel possible mechanism of adipogenesis. Gene 2006;380:137–143
45. Suzuki-Yamamoto T, Nishizawa M, Fukui M, et al. cDNA cloning, expression and characterization of human prostaglandin F synthase. FEBS Lett 1999;462:335–340
46. Bresson E, Boucher-Kovalik S, Chapdelaine P, et al. The human aldose reductase AKR1B1 qualifies as the primary prostaglandin F synthase in the endometrium. J Clin Endocrinol Metab 2011;96:210–219
47. Srivastava SK, Ramana KV, Bhatnagar A. Role of aldose reductase and oxidative damage in diabetes and the consequent potential for therapeutic options. Endocr Rev 2005;26:380–392